The suitability of the Pulnix TM6CN CCD camera for photogrammetric measurement

S. Robson, T.A. Clarke, & J. Chen.

School of Engineering, City University, Northampton Square,
LONDON, EC1V OHB, U.K.

ABSTRACT

The Pulnix TM6CN CCD camera (Figure 1) appears to be a suitable choice for many close range photogrammetric applications where the cost of the final system is a factor. The reasons for this are: its small size, low power consumption, pixel clock output, variable electronic shutter, and relatively high resolution. However, to have any confidence in such a camera a thorough examination is required to assess its characteristics. In this paper an investigation of three of these cameras is described, and their suitability for close range photogrammetry evaluated. The main factors assessed are system component influences, warm-up effects, line jitter, principal point location and lens calibration. The influence of the frame-store on the use of the camera is also estimated and where possible excluded. Results of using these cameras for close range measurement are given and analysed. While many users will have or prefer to buy other cameras, the evaluation of this particular camera should give an understanding of the important features of such image sensors, their use in photogrammetric measuring systems and the processes of evaluating their physical properties.

1. INTRODUCTION

There are a large number of important and interrelated features that can affect the performance of a digital photogrammetric measurement system. The physical characteristics of image sensors will determine which is chosen and a detailed knowledge of the operation of the sensor will determine how the sensor is used. Additionally a thorough awareness of the lens, sensor and framestore interaction and operation is necessary to optimise performance. The rationale behind a physically based understanding of the operation of digital systems is the same as that which was necessary to push film based photogrammetric techniques to their limits. The casual user of such techniques is just as unlikely to produce high quality results as an inexperienced user of solid state sensors. Consequently, until the limiting factors involved are understood, it will be necessary for investigations to be carried out to define component physical properties and their influence within the photogrammetric system.

2. PHYSICAL DESCRIPTION AND EVALUATION OF MAJOR SYSTEM COMPONENTS

2.1 Sensor fundamentals.

There are two types of commercially available solid state image sensors: CCD and CID. The CCD is by far the most common. The difference between these sensor types is the method used to transfer the charge stored at a given pixel site. The development of the CID started in the early 70's, and relies on the photogenerated charge at individual photosites being output directly. The CCD transfers charge, by the manipulation of potential wells, from the generation sites to a position where they are output to an amplifier. The development of the CCD started in 1969 at Bell Labs, U.S.A.[1]. The TM6CN camera uses a CCD sensor [2]so the relative merits of the CID sensor will not be further discussed.

The two common modes of operation of CCD sensors, interline or frame transfer, are another important feature for consideration. The interline transfer sensor (Figure 2) has a column of photosite elements that are adjacent to a shielded shift register. The integration time for the next line takes place as the previous line is clocked out. The Frame transfer sensor moves the entire image from the sensing area to a storage area where it is then read out. The sensor is often blanked from receiving light during the transfer time to avoid continued integration that would result in smearing. The advantage of the interline transfer is that the transfer time (to opaque storage) is short compared to the integration period. For example, in the Pulnix TM6CN[3] camera the transfer time is 64.0μs and the accumulation time is 40.0ms. Both methods of image collection and transfer may also use interlacing, an image transfer method that originated as a means of reducing monitor flicker. In each frame two temporally separated fields are obtained, the odd lines, followed by the even lines.
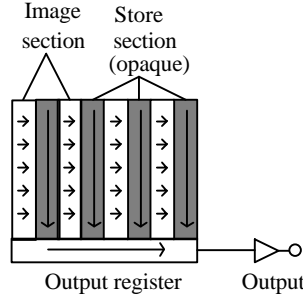
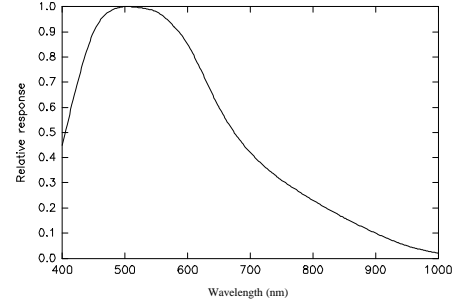Fig.1. The Pulnix TM6CN camera

Fig. 2. Interline Transfer.

Fig. 3. Spectral sensitivity of the Sony
ICX039ALA sensor (including a lens).

When evaluating a particular sensor many terms and features are mentioned, the following description is a simple explanation of the more important terms.

(i) Spectral sensitivity. Silicon absorbs photons in the wavelength range of approximately 200-1100 nm, with a peak sensitivity at 750 nm. Image contrast can change depending on the wavelength. As a consequence many cameras have an optical filter in the optical path to modify the overall response of the system to mimic the response of the human eye. However if a laser beam (e.g. 670 nm) is going to be used as a target, then such integral filters can reduce the intensity of light reaching the chip by an unacceptable amount. There is no filter in the Pulnix TM6CN camera, spectral modification being due to the lens[2] (Figure 3).

(ii) Nyquist's sampling theorem. To recover signal information (in this case an image) in an undistorted form after a sampling process, the original information must be bandwidth limited to half the sampling frequency. As specific spatial filters are not used, sampling above the Nyquist frequency will result in distortions to the image in the form of aliasing. However the lens can be regarded as a spatial filter, since it modulates the frequency of the incident illumination patterns. General purpose C mount lens qualities vary, but the 25 mm f/1.4 Fujinons used in this work appear to be at least comparable to the 58 l mm^{-1} Nyquist limiting value of the sensor (Section 2.2).

(iii) Dynamic range. The dynamic range of a sensor should be greater than the dynamic range of the A-D converter and is defined as the output of a pixel at saturation divided by the RMS noise of that pixel. Typically levels range from 300:1 to 100,000:1 depending on the application. So-called "slow scan" devices often used in astronomy are often designed to have a high dynamic range. The dynamic range of the SONY ICX039ALA chip used in the TM6CN is quoted as 67 dB. The combined Pulnix TM6CN and EPIX SVMGRB4MB framestore response at the two camera gamma settings is shown in Figure 4.

(iv) Charge Transfer Efficiency (CTE). CTE is a measure of the amount of charge transferred from one cell to the next in a CCD sensor. This would be 1.0 if perfect, and typical CTE values vary between 0.9995 - 0.99999 for common devices. The worst case (first pixel in each row) overall transfer efficiency for a 2048 pixel array with a four phase clock is equal to $0.99999^{(2048*4)} = 92\%$. Hence CTE is more important in larger arrays.
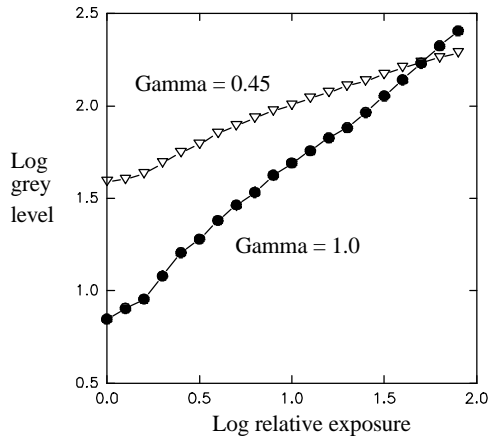

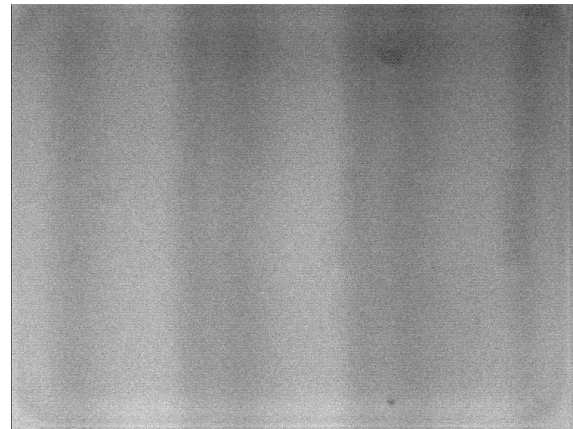Fig. 4. Grey level response at two gamma settings.

Fig.5. Sensor output without lens (greyscale enhanced).

(v) Non Uniformity. This refers to non uniformity in the output signal that can take the form of Fixed Pattern Noise (FPN), noise that is invariant with light intensity, and Photo Response Non Uniformity (PRNU) where the output signal varies in a non uniform way as the light intensity increases. Non-uniformities in the sensor can be caused by variations in substrate thicknesses or pixel element size. However, research has shown[4] that the framestore can itself produce characteristic patterns. A typical pattern was observed for all the Pulnix TM6CN cameras used with the EPIX framestore (Figure 5). This image, taken at a RMS grey level of 180, has been enhanced so that the 4 grey level variations cover a full 0-255 range.

(vi) Geometric variations. The geometric positions of each of the pixels and the relative size of the active areas are all of vital importance in the photogrammetric process. For example sub-pixel target image location may be able to achieve 1/100th of a pixel, however if the physical pixel positions vary then the geometric accuracy will be limited. Fortunately the fabrication process is generally good, such that various investigations have been able to show that the geometric quality of sensors are excellent[5].

| Sensor format	1/2 inch interline transfer CCD
Pixel	752(H)x582(V)
Cell size	8.6(H)x8.3(V) microns
Sensing area	6.41(H)x4.89(V) mm
Dynamic range	67dB
Chip size	7.95 mm(H)x 6.45 mm(V)
Timing.	625 lines, 2:1 interlace (CCIR)
Clock	28.375 MHz
Pixel clock	14.1875 MHz
Horizontal frequency	15.725 KHz
Vertical frequency	50.0 Hz
Video output:	1.0v p-p composite video, 75Ω
S/N ratio:	50 dB min.
Shutter speed:	1/60 - 1/10000 sec.
Minimum illumination:	1.0 lux(F=1.4) without IR. cut filter AGC: On = 16dB standard, Off = 32 dB max.
Gamma:	0.45 or 1
Dimensions:	45 mm (W) x 39 mm (H)x 75 mm (L)

Table 1. Some Pulnix TM6CN camera characteristics.

2.2 Lens fundamentals.

Due to the small area of most CCD arrays, 'C' mount lenses with a typical covering power of 10mm ∅ are commonly used. The 'C' mount specifies: 1" diameter: 33 threads per inch; and a flange image-plane distance of 17.536 mm. For this paper three 25mm f/1.4 Fujinon 'C' mount lenses were used. Several tests were carried out to evaluate the performance of these optics with the Pulnix TM6CN camera. Figure 6 shows some image intensity variations between different camera and lens permutations. For this experiment, an area of white card was evenly illuminated by a pair of lamps positioned at 45° with respect to the card. Small RMS image intensity differences of ±2 grey levels occurred between the different lenses mounted on the same camera body. However the camera sensors demonstrate discrepancies of up to 14 grey levels. Whilst such variations could be removed by adjusting the camera grey balance (a simple matter on the Pulnix TM6CN), the settings should be determined with respect to signal saturation levels. During this experiment, possible image illumination fall-off at the edge of the format using wide apertures was found to be indistinguishable from the ±2 grey value variations present in all Pulnix images. No significant fall off in intensity was found since the Fujinon 25 mm f/1.4 lenses are of standard construction, unlike for example 12.5 mm lenses which are often of retrofocus construction to allow for the 17.536 mm spacing of the C mount standard. Any image intensity variations have implications for photogrammetry if the matching algorithms cannot take account of such shifts and gradients.
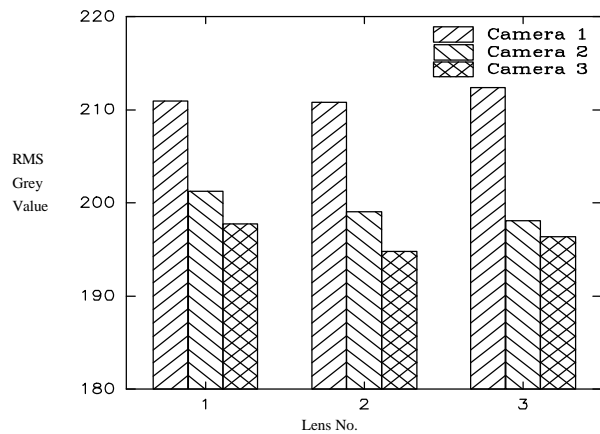
Fig. 6. RMS grey level for three camera/lens combinations.
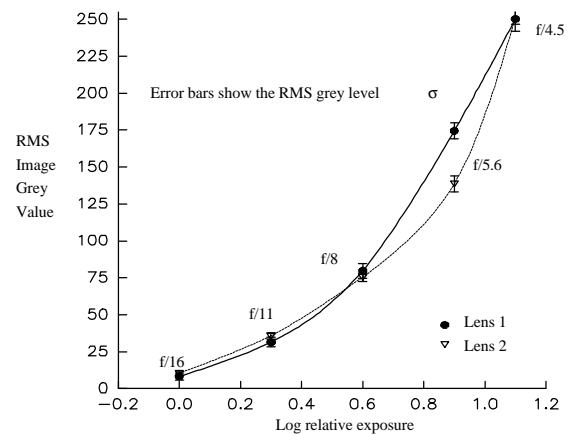
Fig. 7. RMS grey level and lens aperture for two lenses.

Figure 7 demonstrates some results of varying the lens aperture whilst imaging a uniform white card with two different lenses. The only significant difference occurred at f/5.6. Whilst such a difference may not be significant for general applications, in a fully automated measuring system with multiple cameras and automated depth of field control, variations between sensors could be calibrated such that additional radiometric information are included *a priori* in the matching process.

To evaluate system resolution a lens test chart was imaged (Figure 8) at the edge and centre of the image format for each camera and lens permutation. Visual evaluation of the patterns produced at high magnification demonstrated that there was no significant difference between the centre and the edges of the format for all permutations. Figure 9 shows a set of intensity profiles through three sets of line pairs. It can be seen that the spatial resolution of the system is somewhere between 38 and 60 lmm $^{-1}$. Such a value would agree with the 58 lmm^{-1} theoretical maximum resolution given by the Nyquist theorem for the sensor. The variations in resolving power between the three optics tested was found to be insignificant.
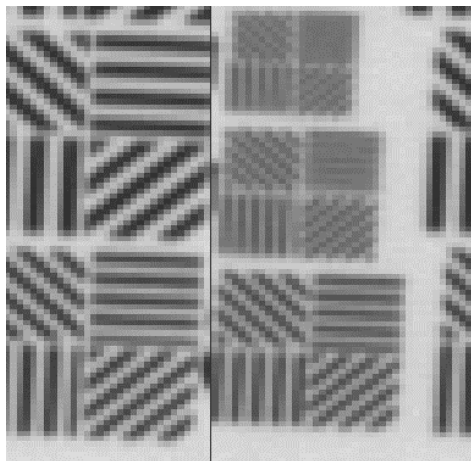

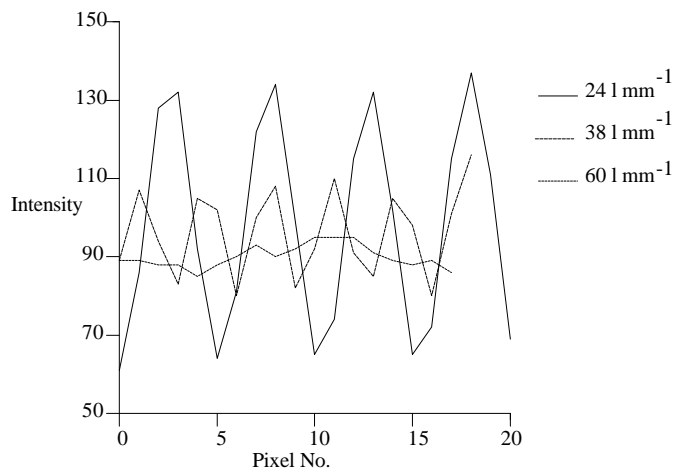Fig. 8. An image of a lens test resolution chart.

Fig. 9. Intensity profiles through three sets of line pairs.

2.3 Framestore fundamentals.

The choice of framestore for photogrammetric close range measurement is likely to be different from that of say, the machine vision researcher or user, where image locations measured in pixels are commonly sufficient. Accurate 3-D measurement necessitates excellent stability over the complete image area because even small localised imperfections can affect the overall measurement precision. Framestore requirements ranked in order of importance may be: (i) pixel clock, therefore a flexible frame grabber is required, (ii) multiplexed inputs, with enough memory on the board to store each image, (iii) software library; if no expertise to program at a low level, or no basic programs of adequate documentation are provided, then this is a necessary accompaniment to the framestore. Many modern framestores have additional features such as: graphics processors; transputers; vga pass through and; single monitor modes. For most photogrammetric requirements such processors are either difficult to program usefully, not powerful enough, or not accessible to the user, hence, they are unlikely to be an essential requirement. The specification suggested so far places the cost of such a frame store into the middle bracket between the cheap, and inflexible versions, and the high priced special purpose boards which may offer features such as: real time histograms; filters and: convolutions. The board selected for the tests conducted for this paper was manufactured by EPIX in the U.S.A. This board, the SVMGRB4MB had six multiplexed inputs, a single pixel clock input, 4Mb of 8 bit memory, and a flexible method of operation. Some of the features of the framestore as it affects the use of the TM6CN camera are:

(i) Pixel clock. The conventional Phase Locked Loop (PLL) method of providing the A-D converter does not provide any method of guaranteeing a one to one correspondence between pixels' intensities provided by the camera, and their supposedly corresponding position in the memory array as measured by the A-D converter. Furthermore the PLL method can give rise to line jitter. The requirement for a pixel clock is discussed in section 3.0.

(ii) A-D converter. There are four main sources of error in A-D converters: quantisation, offset, gain, and linearity. The last three errors are temperature dependent, the converter only functions correctly at its normal operating temperature. All four errors are internal to the A-D converter, and do not include errors caused by incorrect gain, or offset outside the converter. The first error, quantisation, is always present but its effect can be reduced by using the full range of the converter which is 8 bits in the

EPIX framestore. The A-D converter should be matched to the dynamic range of the signal requiring conversion. It would probably benefit the measurement process to have a 10 or 12 bit converter because of the large dynamic range of the camera and the resulting decrease in quantisation error, but to date such framestores are not common.

(iii) Termination. This effect can be demonstrated by imaging a sharp edge or a thin white line on a black background. The resultant image will be the composite effect of: the lens point spread function; the electrical characteristics of the camera; signal transmission between the array and the framestore; and the framestore circuitry. Intensity profiles of two such images are shown in Figures 10a and 10b. The image in Figure 10a was obtained using a 5m 50Ω cable where the phenomenon of ringing can be clearly seen. The cable was replaced by a 2m 50Ω cable to achieve the profile shown in Figure 10b. It should be noted that a longer cable of the recommended 75Ω impedance should achieve results similar to Figure 10b.
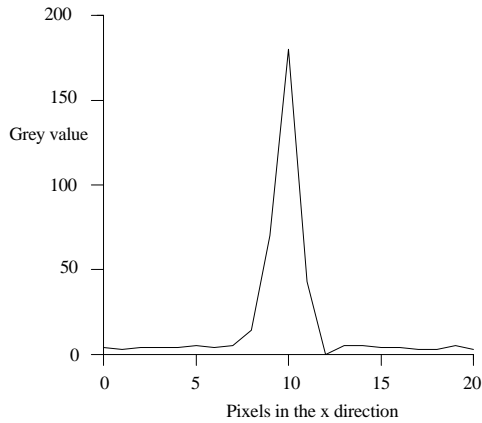

Fig. 10a. Intensity profile of a line using a 5m cable.
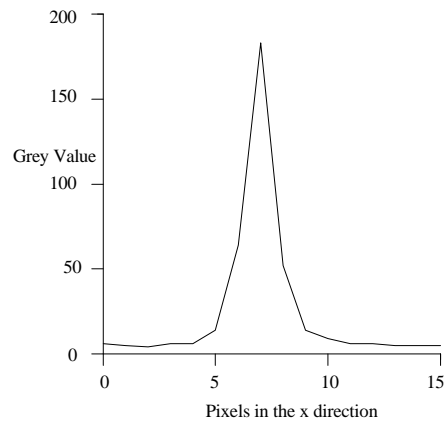

Fig. 10b. Intensity profile of a line using a 2m cable.

2. TEMPERATURE EFFECTS.

The change in temperature of the camera / frame-grabber combination has been shown to influence image acquisition[6]. To analyse this, a number of tests were performed. By allowing the camera and the framestore to warm up at differing times the effects attributable to each were isolated and determined. A test field consisting of sixteen circular retro-reflective targets stuck onto a plane glass slide that had been sprayed matt black was constructed. The targets were arranged to cover the entire field of view of the camera as shown in Figures 11 and 12. The test field and camera were then firmly fixed onto an optical bench. The test plane was surrounded by black paper to remove the influence of any outside stray light and a light source was placed behind the camera. In this way the retro-reflective targets could produce a high signal to noise ratio image. The distance from the test plane to the camera was set at approximately 665 mm. At this distance each target image point would fit into a 21 x 21 pixel block. Once the required imaging conditions were obtained all components were fixed rigidly together .
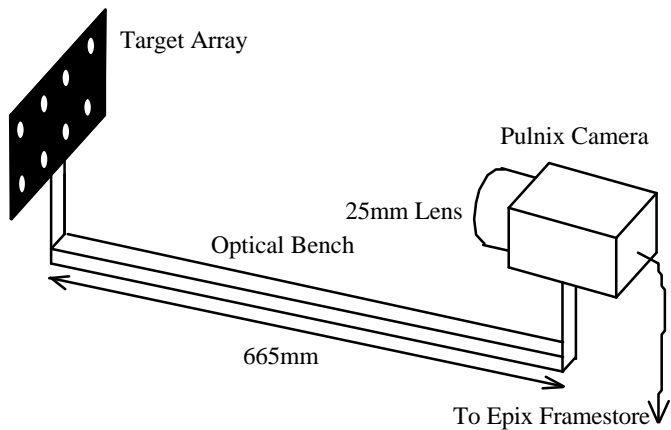
Fig. 11. The test field configuration used for the warm-up investigation.
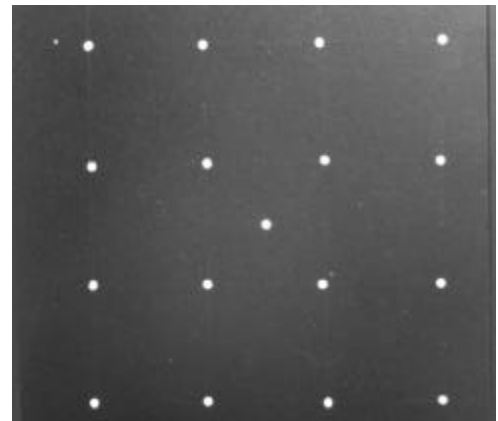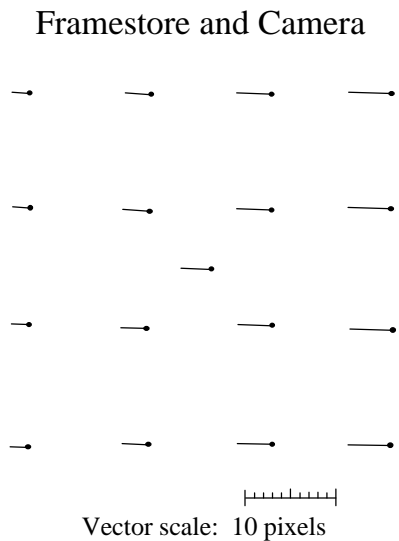

Fig. 12. An image of the test field.

Framestore and Camera

Vector scale: 10 pixels

Fig. 13a. Vectors of warm-up of the camera and framestore in a 60 minute period.

Framestore
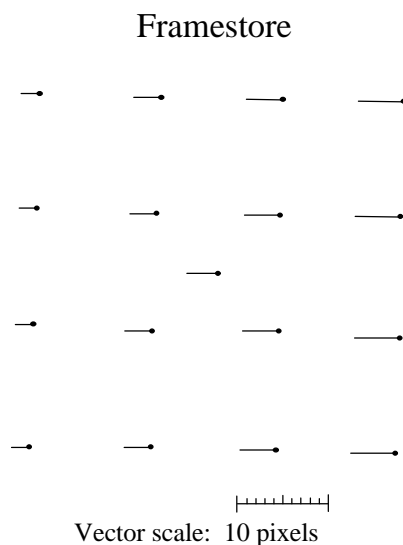

Vector scale: 10 pixels

Fig. 13b. Vectors of warm-up of the framestore in a 60 minute period.

Initially the EPIX frame grabber and a Pulnix camera were switched on together. A series of images were collected over a period of time. The targets in each image were located by a centroid subpixel location algorithm, in which a 25 x 25 rectangular pixel window was used. This algorithm can provide a precision of 1/50 of a pixel given good quality images. The x and y image co-ordinates were stored such that any time or temperature related changes in the co-ordinates of the targets could be plotted and analysed. The largest variation of the co-ordinates was found to be at target locations on one side of the image (Figure 13a).
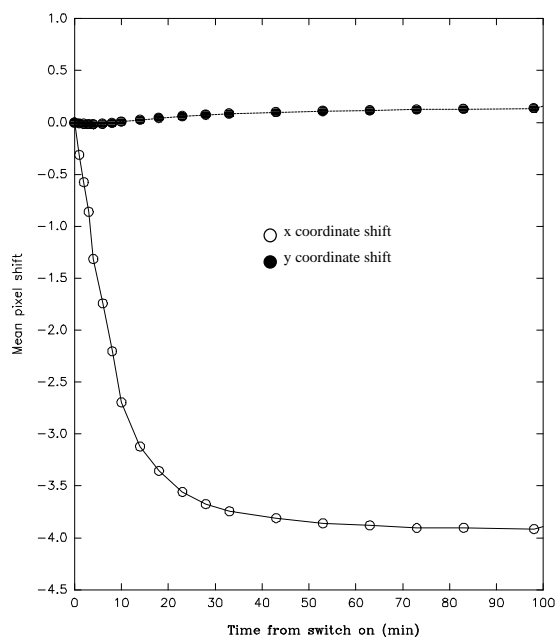

Fig. 14a. The RMS x, y co-ordinate shift of all targets over the period of warm up for both the camera and framestore.
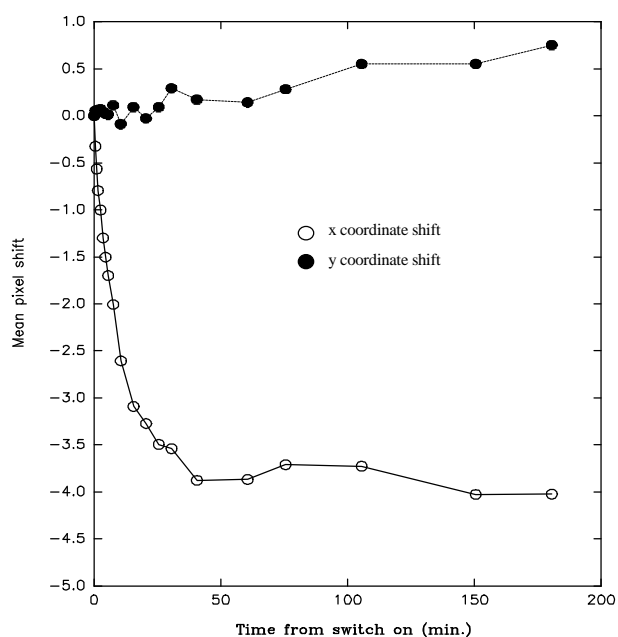

Fig. 14b. The RMS x, y co-ordinate shift of all targets over the period of warm up of the framestore.

A significant shift in the co-ordinates of all the targets can be observed during the period when the camera and frame grabber are warming up. This shift is predominantly in the x co-ordinate direction. The co-ordinate variation became stable after approximately 60 minutes. The total RMS warm-up shift was as large as 4 pixels (Figure 14a). However the experiment does not allow any conclusions to be drawn concerning the source of the effect. Hence, two further tests were conducted to isolate the temperature warm up effects of each of the three cameras available and the EPIX framestore. These tests were conducted exactly as before except either the frame grabber or camera was stabilised over a two hour period before the other component in the system was switched on. Again image co-ordinates were collected at regular time intervals. The results of these experiments are shown in Figures 13b, 14b, 15 and 16, where it can be seen that the temperature related drift in the camera alone is very small and similar in both x and y co-ordinate directions. However the large (4 pixel) warm-up change exhibited earlier, is present only
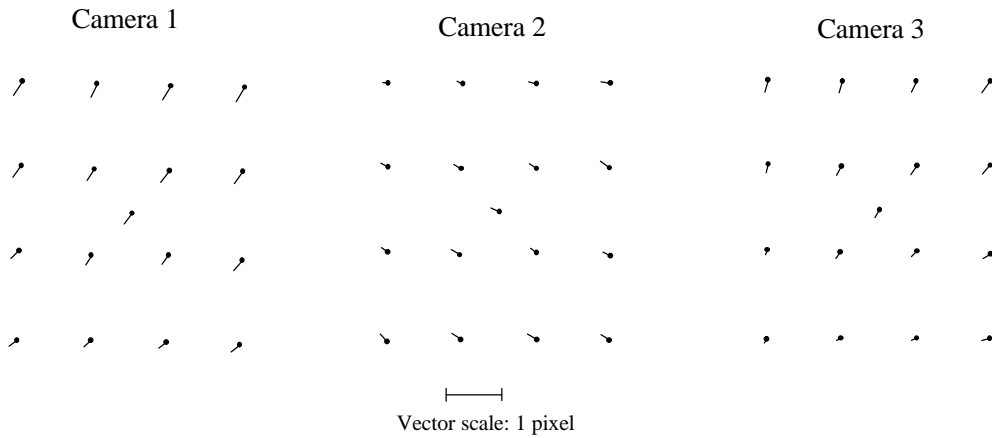
Camera 1   Camera 2   Camera 3

Vector scale: 1 pixel

Fig. 15. Image co-ordinate change for the first 60 minutes of warm-up for each Pulnix camera.

Pulnix TM6CN camera warmup

x coordinate shift   y coordinate shift
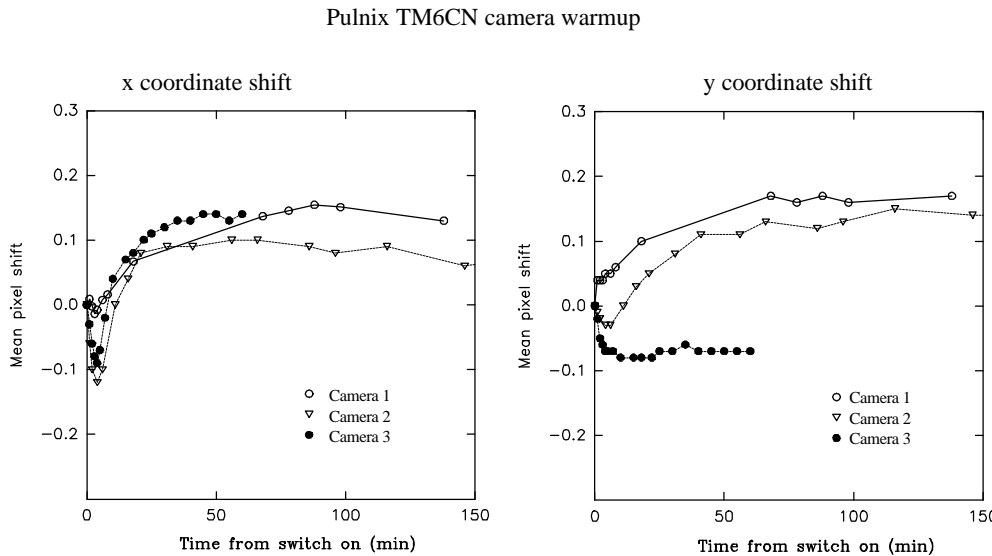
Fig. 16. RMS x, y co-ordinate shift for all targets over the period of the camera warm-up test.

during the warm-up of the framestore. Since the change is in the x co-ordinate direction only it must be due to a variation of the frequency of the clock signals generated by the framestore. The shift can be modelled by an affine transformation, yielding image co-ordinate residuals of 1/50 of a pixel. Warm-up effects for the three cameras demonstrate changes of up to 1/5 pixel. These changes are of the same order of magnitude as would be expected from a thermal expansion of the silicon CCD array. After modelling by an affine transformation the image co-ordinate residuals again approached 1/50th of a pixel.

The conclusions that may be made concerning the warm-up effects are scale changes in the x co-ordinate direction are largely frame store related and should not occur with the pixel clock in use. However they can be modelled in practice. Small additional linear image co-ordinate changes, probably due to sensor thermal expansion, occur during camera warm-up.

3. LINE JITTER.

The causes of line jitter are well known[4,7]. The problem originates from the video data transfer standard originally devised for Vidicon cameras that do not have discrete pixels so the output is a continuous function of the time taken for the electron beam to sweep the sensing area. Hence, the initial standard used for data transfer between the camera and the framestore had no timing synchronisation between the sensor output and the A-D converter conversion period. In the case of the CCD sensor, discrete pixels are the originators of a voltage train. The camera clocks the analogue image intensity data from the CCD sensor at a fixed frequency (14.3 MHz for the CCIR standard). Many framestores use a Phase Locked Loop (PLL) to control the timing of the A-D converter based on the frequency that is expected. The timing of the conversion takes place at a given number of clock periods after the beginning of a horizontal line that is determined by a transition in the timing signals that are encoded with the image information in a composite synchronisation signal. Any variation in the ability to determine the start of this period gives rise to line jitter. Line jitter is independent of another potentially serious problem, that of clock period variations between camera and framestore, as described in the series of warm-up tests. Since the CCIR output is an analogue voltage train and the two timing systems are completely independent of each other (apart from the horizontal and vertical synchronisation pulses) there is no accurate correspondence between pixel intensity and the A-D conversion period. It is possible for the output of a 752 pixel sensor to be sampled by a 512 x 512 framestore at a different frequency (e.g. 10 MHz), with apparently successful results, conversely, the output from a 752 pixel sensor may be over-sampled, producing an image of superficially higher resolution.

There are two possible methods of solving the linejitter problem. One is to synchronise the data output from the camera with the framestore, and the other is to average results over many frames. This former is achieved if the camera has a pixel clock output and the framestore can accept a pixel clock input. A disadvantage with some framestores that allow flexible input of signals from cameras is that they often require the camera horizontal and vertical signals in addition to the pixel clock pulses. The EPIX SVMGRB4MB framestore allows the use of horizontal and vertical synchronisation pulses with the camera pixel clock, albeit with some electrical alterations to the framestore card.

To analyse the extent of line jitter a test field was constructed consisting of an array of stretched white lines imaged against a black velvet background. Lighting was optimised to provide even illumination across the test field, but with sufficient light to obtain optimum imaging conditions for automated subpixel location. Image co-ordinate data for the eight lines within each single frame was computed using a subpixel algorithm. Twenty-seven images were taken using all possible camera and lens permutations at three different distances. The experiment was then repeated with the camera rotated by 90° to produce fifty-four images in total. For each image, subpixel image co-ordinate data were computed at eighty positions on each of the eight imaged lines. Each horizontal and vertical image pair were combined in a lens distortion calibration[8]. By these means the systematic effects of radial and tangential lens distortion were removed from the co-ordinate data. Some results of the lens calibrations are discussed in section 5. The residuals from the calibration data represent the errors present in the imaging system (Table 2).

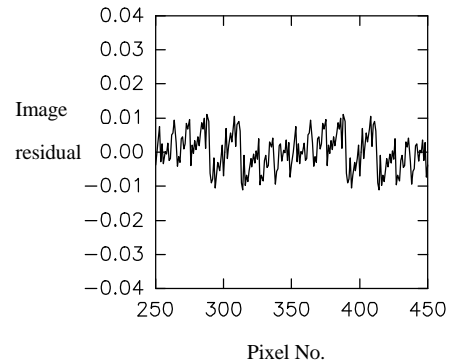| RMS image residual (σ)	σx	σy
μm	0.341	0.291
pixels	1/25	1/28

Table 2. RMS image co-ordinate residual standard deviations for all 54 images.

Although there is a small difference between the x and y co-ordinate residuals, there is insufficient evidence to attribute the difference to line jitter. On analysing the individual images in detail it was observed that some of the lines only covered about four to five pixels, there were small variations in illumination and some ringing was present. These and other error sources such as image quantisation and thermal effects will have contributed to the residuals computed by the lens calibration routine. Consequently these mean residual standard deviations represent the total error budget, the effect of line jitter alone cannot be quantified.

To analyse the system further, two images which did not exhibit any of the degradations mentioned previously were selected. Care was taken to minimise lens distortions by positioning a line to coincide with the optical axis of the lens. A linear regression was performed using only data computed from the central region of the line. Residuals from both horizontal and vertical lines are shown in Figures 17a and 17b.
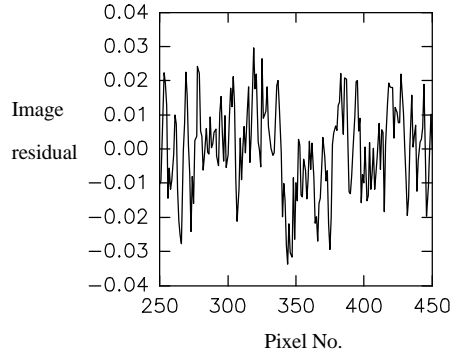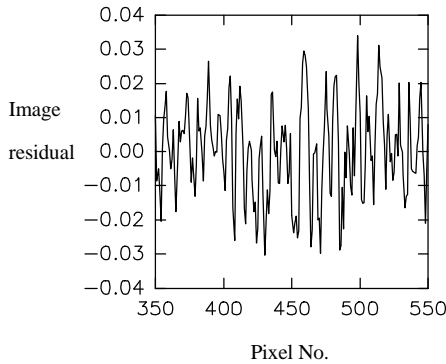
Fig. 17a & 17 b Sub-pixel residuals in the x and y directions.   **Fig. 17c. Quantisation error for a similar line.**

The results obtained can be compared to the theoretical limit imposed by the quantisation error (Figure. 17c) where it can be seen that the quantisation error accounts for at least one third of the total error. Interestingly no significant differences in the x and y directions attributable to line jitter can be seen using the Pulnix TM6CN and EPIX framestore. Analysis of the image co-ordinate residuals from a self-calibrating bundle adjustment carried out in section 6 of this paper (Table 6) do not demonstrate any significant differences in magnitude between the x and y image co-ordinate residuals. It should be mentioned at this point that the bundle technique is not considered to be a particularly valid technique for evaluating line jitter, since the network and least squares process have a direct bearing on the relative magnitudes of the image residuals. For a complete evaluation, these

results must be compared to the same system with pixel clock synchronisation. An investigation of the pixel clock output signal from the camera revealed that it was not TTL compatible (0 < 0.8V, 1 > 2.4V). The camera provided a signal with an amplitude of one Volt offset from ground by one Volt. Unfortunately the conversion of the signal was not completed in time for inclusion in this paper. It appears that line jitter is not a serious problem with this system when compared to other error sources. However the inclusion of the pixel clock is expected to provide significant benefits in reducing warm-up effects and improving image stability.
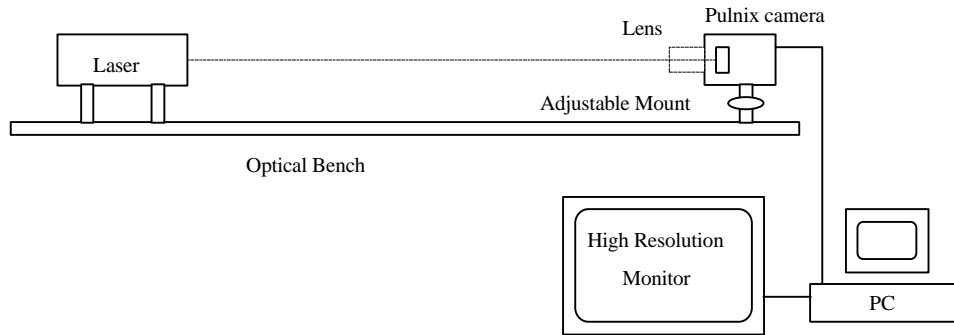
4. PRINCIPAL POINT.

Fig. 18. Schematic diagram of the principal point location system.

The principal point of symmetry was determined by direct optical measurement for each of the camera and lens combinations. The method used was based on a method presented by Burner *et al* [9]. A low power laser was aligned with the centre of the CCD array by causing the primary reflection from the surface of the sensor to coincide with the incident beam (Figure 18). Coincidence was identified by symmetry with the diffraction pattern caused by the surface structure of the sensor. Care had to be taken in distinguishing this from the similar strength reflection from the cover glass front surface. Each lens was fitted to the camera and an image grabbed with the laser suitably attenuated. The location of the laser imaged spot by definition coincides with the principal point of symmetry.

Initially a principal point determination repeatability test was conducted. Three operators repeatedly aligned the system using camera 2 and lens 2 focused at infinity. In each case the target image centre was located by visual examination of the image co-ordinate grey values. Results from this evaluation (Table 3.) show good repeatability between operators. The same method was then used to assess the principal point of symmetry for each camera and lens combination, mean values are shown in (Table 4).

Operator	1		2		3	
Observation	**x**	**y**	**x**	**y**	**x**	**y**
1	350	219	350	219	349	219
2	351	218	349	219	348	218.5
3	351	219	349	219	349	218.5
4	351	218.5	351	219	348	218.5
5	351	218.5	349.5	219	348	218.5

Camera	Lens	Principal Point	
No.	No.	x	y
1	1	360.5	268
1	2	354	263.5
1	3	343	275.5
2	2	351	221
3	3	346.5	293

Focus Setting	x	y
Infinity	350	220
5m	349	218.5
2m	348.5	216.5
1m	349	213.5
0.5m	347	206
Infinity	350	220.5

Table 3. Lens principal point location repeatability.   Table 4. Principal point measurement.   Table 5. Variation of lens focus.

In an automated measurement system, lens focusing may be carried out automatically. It is well known that in a real lens the principal point will vary with the lens extension necessary to achieve sharp focus. Such variations were evaluated for one of the cameras by adjusting the lens to five different settings throughout its imaging range. Results are shown in table 5, significant variations of 3 pixels in x and 14 pixels in y were noted. Since the principal point parameters estimated by bundle adjustment are often highly correlated with camera rotations and tangential lens distortion, it is highly recommended that appropriately weighted *a priori* observations from direct measurement are included in the adjustment process.

5. LENS CALIBRATION.

Lens distortion can be thought of as the deviation of the image ray from ideal collinearity with the object ray. For a perfect lens, each object point will project in a straight line through the lens perspective centre to produce an image. However no lens has perfect behaviour and will always have imaging aberrations. Geometric lens distortion is usually divided into two types, radial and tangential. As the name implies, radial distortion affects the position of image points on a straight line radiating from the principal point. The magnitude of tangential distortion varies as a function of the radial distance and the orientation of the imaged point to the principal point with respect to a reference direction. Functions describing the magnitude of the lens

distortion components can be written (Brown 1981) such that any image co-ordinate deformation caused by the optical system can be corrected.

The image set obtained during the line jitter experiments was used to calibrate the three lens and camera combinations. The builder's chalk line used was white, strong and flexible. The only disadvantage was that it was woven from fine threads which could be resolved by the camera at distances of about 0.5 metres prohibiting accurate assessment of lens distortion below about 1m. Image sets were collected at object distances of 4m, 2m and 1m. Eight lines were imaged using each of the three cameras. Results of the calibrations are detailed in Figures 19a, 19b, 19c for the radial lens distortion and 20a, 20b and 20c for the tangential lens distortion.
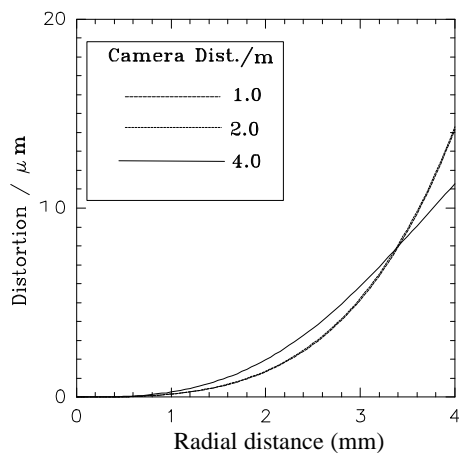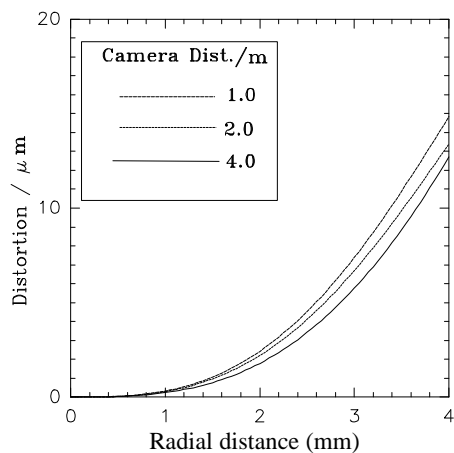
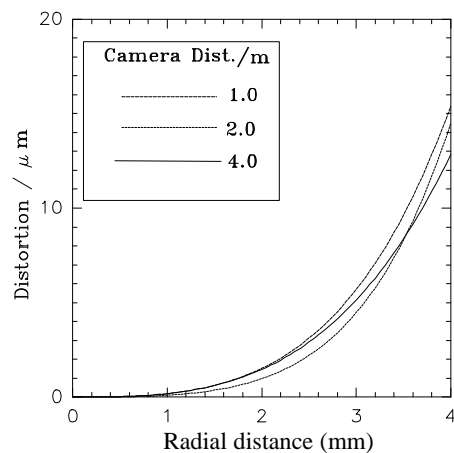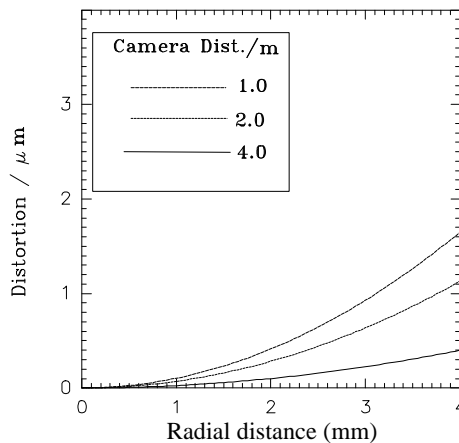**Fig. 19a Camera 1, lens 1.** **Fig. 19b Camera 2, lens 2.** **Fig. 19c Camera 3, lens 3.**
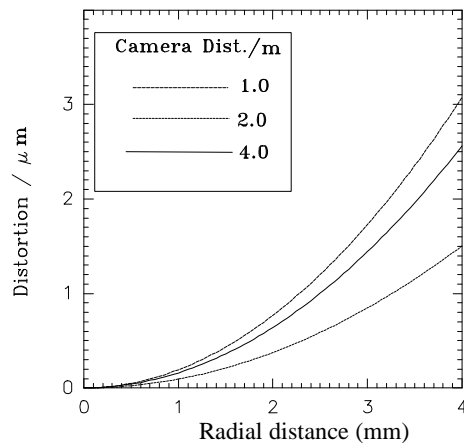
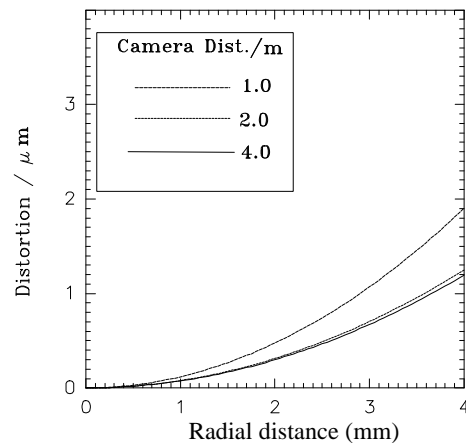**Fig. 20a Camera 1, lens 1.** **Fig. 20b Camera 2, lens 2.** **Fig. 20c Camera 3, lens 3.**

Radial lens distortion is primarily represented by the k_1 component. Variations in the shape of the lens distortion curves with object distance show differences of up to 3 μm at the format extremes. However these discrepancies are insignificant given the standard deviations of the parameters estimated by this experiment. Tangential distortion is approximately seven times smaller in magnitude than the radial component. For engineering applications it is often necessary to attain sub-pixel measurement accuracies of at least 1/30th of a pixel (0.3μm), consequently both changes in radial lens distortion with object distance and tangential lens distortion parameters will be significant. These parameters must be included by an *a priori* method since multiple single camera networks do not provide a good calibration situation, the use of parameters constrained by their standard deviations is suggested.

6. PHOTOGRAMMETRIC EVALUATION.

To assess some of the system parameters investigated during this paper, a self calibration was carried out. A testfield for the calibration was provided by an object which was the subject of a current experiment. The self calibration was performed using all three cameras with their respective lenses, in the configuration shown in figure 20, to image a wooden board on which were placed 74 circular retro-reflective targets. By virtue of the GAP bundle adjustment program and an automated target matching procedure, both developed at City University, the calibration could be performed automatically.
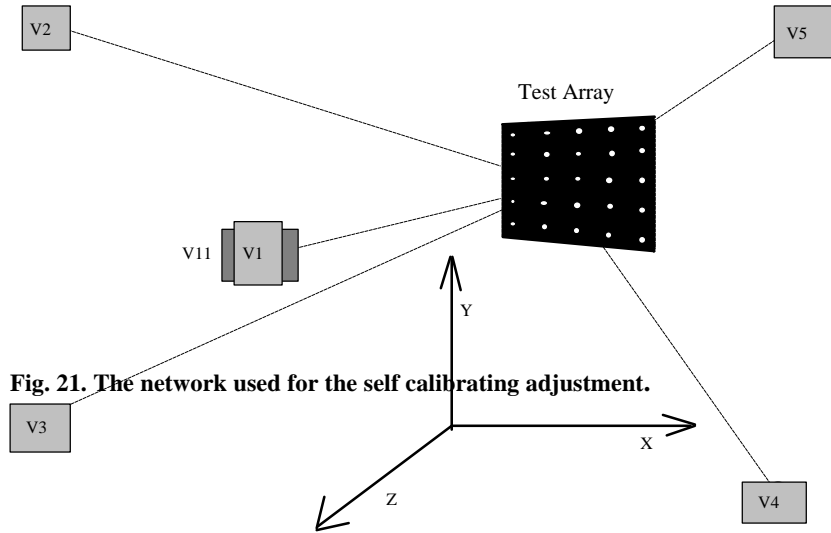
Fig. 21. The network used for the self calibrating adjustment.

A free adjustment using 6 images per camera such that all 74 targets were imaged at each viewpoint was computed. Camera calibration was carried out for f, x_p, y_p, and lens parameters k_1, p_1 and p_2 for each individual camera. The principal point shifts from the laser alignment were used as *a priori* values constrained by a standard deviation of 3 pixels. All three image sets were combined in a single adjustment with individual camera calibration, such that the 1332 photo-co-ordinate measurements gave rise to 2329 degrees of freedom. Target images were located to subpixel accuracy using a centroid method. These image co-ordinates were then downloaded into the 3D matching procedure to automatically obtain correct target correspondences. The adjustment was then processed using City University's GAP program to give a self-calibrating free adjustment.

Degrees of Freedom 2329		σ_0^2 : 0.303		**No. Measurements** 1332
Co-ordinate axis	X		Y	Z
Target RMS σ	0.0163 mm		0.0210 mm	0.0207 mm
Image RMS residual	0.53μm (1/16 pixel)		0.49μm (1/17 pixel)	---------

Table 6. Some parameters from the self-calibrating free bundle adjustment.

Combination	**Focal Length** (mm)	**X_p** (mm)	**Y_p** (mm)	**k1**	**p1**	**p2**
Camera 1, Lens 1	25.107	0.096	0.041	-163.56	-0.050	-0.041
Camera 2, Lens 2	25.022	0.151	0.515	-142.40	-0.070	-0.132
Camera 3, Lens 3	25.011	0.176	-0.066	-132.30	-0.161	-0.017
Standard Deviation	0.010	0.008	0.008	9.57	0.006	0.007

Table 7. Some camera calibration parameters and their standard deviations for the Pulnix camera/lens combinations.

The adjustment results show good correlation with the principal point offset and tangential lens distortion coefficients estimated in sections 4 and 5. The radial distortion values are however significantly different, this discrepancy being attributed to several targets at the edges of the wooden test array which had small background intensity values giving rise to sub-pixel estimation errors. Such observations were automatically marked as having significant residuals by GAP and could be either measured using a refined algorithm of discounted from the solution, however for the purposes of this evaluation this was decided to be unnecessary and was not carried out. The calibration has demonstrated that high precision results can be obtained using small numbers of digital images given an *a priori* knowledge of the performance of individual elements of the digital imaging system.

8. CONCLUSIONS.

In this paper the fundamental characteristics of CCD cameras such as the Pulnix TM6CN camera have been described. Tests to isolate the warm up effects of camera and framestore revealed: i) that timing differences between camera and framestore can be

significant during a warm-up period and; ii) a small but significant co-ordinate variation could also be detected which may be attributed to thermal expansion of the sensor chip. Line jitter, a significant feature in other investigations, was not found to be distinguishable from other error sources, in fact no significant difference was found between the x and y co-ordinate directions in any of the experiments carried out. The investigation into the location of the principal point revealed that there was a significant co-ordinate difference between the principal point and the centre of the array. Lens calibration demonstrated that k_1 was the dominant factor, this was borne out in the self calibration where the k_2 and k_3 terms were insignificant. The combination of Pulnix TM6CN camera and EPIX framestore has provided a photogrammetric solution which is able to provide comparable object space precision to that obtained by other workers. As a consequence of the work carried out for this paper it is hoped that physical models and better techniques will be developed to improve the precision and reliability of the system as a whole. Explanations for the image co-ordinate variations seen must be developed if precision and reliability are to be improved. In conclusion the Pulnix TM6CN camera appears to be well suited to close range photogrammetric use, but cannot be viewed in isolation from the framestore. The system at City University has been successfully applied to a wide variety of engineering applications.

9. REFERENCES.

1. Tseng, H., Ambrose J.R. and Faltahi, M. "Evolution of the Solid State Image sensor.", Journal of Imaging Science, Vol 29, No 1, Jan/Feb, 1985.

2. SONY. Semiconductor IC Data book 1991, CCD cameras and peripherals. 862pp. Pub. Sony Corporation, Tokyo 108, Japan. 1991.

3. PULNIX. TM6CN Operations and maintenance manual. Pulnix America inc. 27pp 770 Pub. Pulnix Inc, Lucerne drive, Sunny Vale, CA 94086. 1992.

4. Beyer H.A. "Geometric and Radiometric analysis of a CCD-camera based photogrammetric close range system". PhD thesis ETH-Honggerburg CH-8093 Zurich, 186pp. ISBN 3-906513-24-6. May 1992.

5. Lenz, R. "Image data acquisition with CCD cameras." Optical 3D measurement techniques, applications in inspection, quality control and robotics. Ed. Gruen & Kahmen, p.22-34. Pub. Weichmann,Vienna. September 18-20 1989.

6. Wong , K.W, Lew. M. and Ke Y. "Experience with two vision systems." Close Range Photogrammetry meets machine vision. SPIE Vol 1395. p.3-7 Zurich. 1990.

7. Raynor, J.M. and Seits, P. "The technology and practical problems of pixel-synchronous CCD data acquisition for optical metrology applications." Close Range Photogrammetry meets machine vision. SPIE Vol 1395 p. 96-103. Zurich. 1990.

8. Fryer, J. G. "Camera calibration in Non-Topographic photogrammetry," Chapt 5, Non Topographic Photogrammetry, edited by H. M. Karara, 2nd ed., pp59-69, Pub. ASP&RS, Falls Church, 1989.

9. Burner, A.W., Snow W.L., Shortis M.R. and Goad W.K. "Laboratory calibration and characterisation of video cameras." Close Range Photogrammetry meets machine vision. SPIE Vol 1395. p. 664-671. Zurich. 1990.

PAPER REFERENCE

Robson, S. Clarke, T.A. & Chen, J., 1993. The suitability of the Pulnix TM6CN CCD camera for photogrammetric measurement. SPIE Vol. 2067, Videometrics II, Conf. "Optical tools for manufacturing and advanced automation", pp 66-77.